A Close-Approach Solar Probe Design Feasibility and Mission Study

J. G. LUNDHOLM JR.,* E. S. PROHASKA,† S. HOYER,‡ AND J. AVERELL§
Avco Corporation, Wilmington, Mass.

A probe to approach the sun to a perihelion distance of three solar radii is shown to be scientifically desirable and feasible within the next two decades. This probe will perform measurements of the coronal magnetic field, coronal bulk flow patterns, and super-thermal particles. The mission will utilize nuclear-electric propulsion with a simple thrusting program. The final orbit is highly elliptical and does not require thrust to be applied at distances too close to the sun for operation of a 500-kwe SNAP-50-type nuclear-electric system. The electrically propelled spacecraft that transports the sun orbiter contains power, propulsion, attitude control, command, and communications systems, as well as a system to separate the orbiter from the spacecraft. At the conclusion of powered flight, the sun orbiter is separated from the propulsion system and is completely self-sufficient. The gross initial weight of the spacecraft is 28,330 lb, of which 1450 is attributed to the orbiter.

Nomenclature

A_s = orbiter shield area
A_x = orbiter cross-sectional area presented to the sun
e = eccentricity (orbital)
F = engine thrust, lb
F' = configuration factor
f_r = fraction of thrust in radial direction
f_θ = fraction of thrust in circumferential direction
GM_0 = 1.32×10^{11}, km^3/sec^2
g_0 = acceleration of gravity at the earth's surface, ft/sec^2
q_s = solar constant at one a.u. from the sun, 440 Btu/ft^2-hr
I_{sp} = specific impulse, sec
I_{sp}' = specific impulse, sec $\times 10^{-3}$
n = number of shields
P_b = beam power, kw
P_b' = beam power, kw $\times 10^{-2}$
R = radius of intermediate shields
r = nondimensional radial coordinate from the sun, a.u.
r' = radial coordinate, km
r_p = perihelion distance (instantaneous)
T = nondimensional thrust
T' = temperature, °R
T_b' = temperature of adiabatic wall
T_i' = temperature of first shield
t = nondimensional time, $\frac{1}{2}\pi$ yr
t' = time, sec
t_e = one-nondimensional time unit, $\frac{1}{2}\pi$ yr
V_e = velocity of the earth, fps
v_e = electric engine exhaust velocity ($g_0 I_{sp}$), fps
v_r, v_θ = radial and circumferential velocities of the probe
Δv = velocity increment, fps
W_d = gross dry weight of solar probe
W_i = initial gross weight of solar probe, lb
W_i' = initial weight, lb $\times 10^{-4}$
W_p = initial weight of propellant
$\dot{W}_p$ = dw/dt = rate of weight loss due to propellant consumption
x = spacing between shields
α = nondimensional velocity, v_e/V_e
β = nondimensional weight loss rate parameter $(t_e/W_i)/|dw/dt|$
α' = absorptivity
ϵ = surface emissivity
ζ = tankage factor
θ = azimuthal angle, rad
θ_0 = azimuthal angle of instantaneous aphelion
θ_c = orbiter cone angle
θ_s = angle subtended by the sun
λ = wavelength
σ = Stefan-Bolzmann constant
ψ = emissivity configuration function

Introduction

THE sun exerts a profound influence on planetary atmospheres and surfaces and on the interplanetary medium. A thorough knowledge of the sun is therefore indispensible for an understanding of our environment in space, of solar-terrestrial relations, and of solar-planetary relations. The study of the sun is naturally of great scientific interest. Because it is in many ways a typical star, investigations of the sun provide valuable data in the fundamental astrophysical problem of determining the structure and evolution of stars.

Our present knowledge of the sun is wholly indirect in the sense that it is derived primarily from measurements, at the earth, of the solar electromagnetic spectrum. Observational data referring to material particle emission from the sun are quite fragmentary and incomplete. In particular, in this latter respect, the development of solar probes offers an exciting prospect. Such a probe would permit direct measurements in the solar atmosphere and particularly in regions where the existing indirect methods are either inaccurate or inapplicable. Moreover, it would permit measurements of a kind that now are not accessible even by indirect methods. A high priority must be assigned to the measurement of the magnetic field. Such measurements should provide data on the spatial geometry, magnitude, and direction of the field and should be made with sufficient frequency to provide information about temporal fluctuations. Priority is also placed on the observation of superthermal particles. Desirable information would relate to particle types, densities, energy spectra, directionality, and fluctuations. Measurements of density, temperature, and flow velocity of the coronal material would also be extremely valuable.[1,2]

Presented at the 1st AIAA Annual Meeting, Washington, D. C., June 29–July 2, 1964; revision received January 29, 1965. The authors wish to acknowledge the assistance and many valuable suggestions received from T. Gold, M. Krook, A. C. Maliaris, K. W. Wreghitt, R. A. Cocozella, R. S. Bartle, R. A. Atwood, E. G. Wolff, D. W. Grunditz, M. S. Koslover, P. Kachmar, I. Most, N. Lindsay, and S. Stodowski.

* Project Manager, Advanced Space Systems, Research and Advanced Development Division; now Director, Advanced Research and Technology Department, Space Systems Division, Fairchild Hiller Corporation, Rockville, Md. Associate Fellow Member AIAA.

† Senior Staff Engineer, Advanced Space Systems.

‡ Senior Staff Engineer, Advanced Space Systems; now Project Engineer, Advanced Research and Technology Department, Space Systems Division, Fairchild Hiller Corporation, Rockville, Md. Member AIAA.

§ Staff Scientist, Research Directorate.

Solar plasma and magnetic fields are connected with most solar phenomena. Our knowledge of the solar magnetic field is derived from measurement of the Zeeman effect for lines in the optical region of the spectrum. Since these lines are formed in an essentially thin layer at the top of the photosphere, very little is known about the fields above the photosphere. A variety of magnetic-field configurations can be suggested to account for the origin, storage, escape, and propagation of energetic charged particles from the sun. At distances greater than approximately 10 solar radii from the photosphere, it is probable that various interactions have so obscured the original magnetic-field configurations that no conclusive results can be deduced from the data. This is one reason why it has been concluded that the probe must go to three solar radii.

The feasibility of the mission hinges on finding solutions to two critical requirements: a propulsion system capable of placing the payload in an orbit with a perihelion of 3 to 10 solar radii and a thermal protection system for the payload.

The Launch Vehicle

The availability of suitable launch vehicles is very limited. No launch vehicle now in development is capable of placing an orbiter of suitable size in the desired orbit by chemical energy alone[3] (Fig. 1). Although the Saturn V configuration, even with multiple upper stages, does not have the capability of injecting the orbiter of adequate size directly into the desired orbit, it easily can boost an ion-propelled spacecraft to earth-escape velocity. The Saturn V launch vehicle configuration is specified to have a capability of lifting 90,000 lb to earth-escape velocity (37,000 fps). This is more than adequate to inject a 28,340-lb nuclear-electric, ion-propelled solar probe into an earth-escape trajectory that will meet the initial orbit requirements of a suitable low-thrust trajectory. (The possibility exists of utilizing the excess Saturn V capacity to give the spacecraft an additional velocity increment after earth escape to improve the initial conditions for the low-thrust trajectory. Time has not permitted an investigation of this possibility.)

Trajectory and Propulsion

Trajectory analyses were made for several thrusting programs, including continuous and programed low thrust as well as several for impulsive[4] thrust. The only program found to be feasible was one in which the thrust vector is directed in a circumferential direction normal to the radius

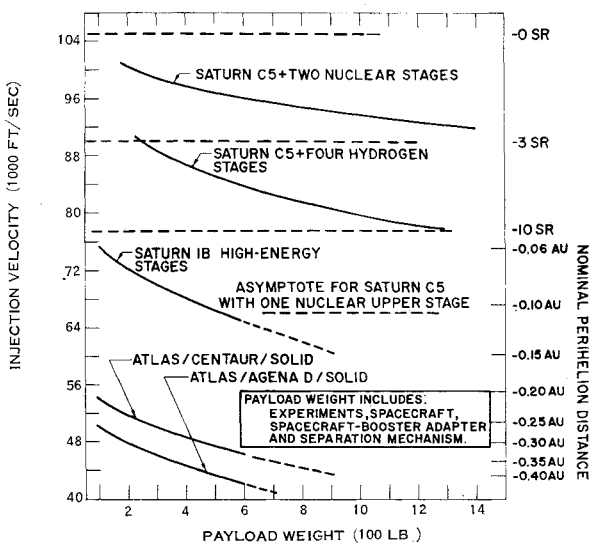

Fig. 1 Launch: vehicle capabilities.

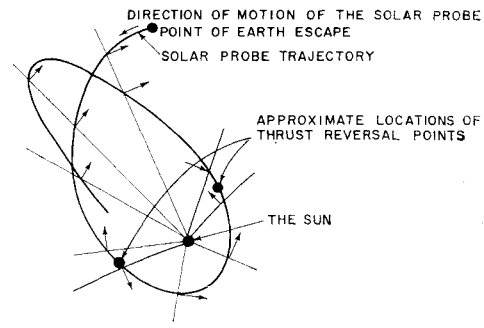

Fig. 2 Flip thrust program (direction of thrust is indicated by arrows).

vector to the sun. This thrust is flipped back and forth a limited number of times, giving rise to the name "flip thrust" for this program (Fig. 2). The thrust is applied so as to produce a highly elliptic final orbit with the desired perihelion distance without passing close enough to require solar thermal shielding of the propulsion unit during the powered phase of the trajectory (Fig. 3).

The nondimensional trajectory equations are

$$\ddot{r} - r\dot{\theta} = (1/r^2) + f_r T \tag{1}$$

$$r\ddot{\theta} + 2\dot{r}\dot{\theta} = f_\theta T \tag{2}$$

where

$$T = -\alpha\beta/(1 - \beta t) \tag{3}$$

$$\alpha \equiv v_e/V_e \qquad \text{and} \qquad \beta \equiv (t_e/W_i)|dw/dt| \tag{4}$$

The thrust is applied normal to the sun-probe line and is programed in a manner such that, in the aphelion region, the tangential velocity is reduced, but in the perihelion region it is increased. That is, $f_r = 0$ and $f_\theta = -(\ddot{r}/|\ddot{r}|)$. Thus, retrothrust is applied to the spacecraft after escape from the earth's influence in the plane of the trajectory until the instantaneous radial acceleration becomes zero. At this point, the circumferential thrust is reversed and applied to increase the circumferential velocity (and, as a result, the eccentricity and aphelion distance) until the radial acceleration gain becomes zero. Here, the thrust is again reversed and retrothrust applied once more. A retarding thrust is applied whenever the radial acceleration is negative and an accelerating thrust whenever the radial acceleration is positive. Positive thrust in the plane of the trajectory in the perihelion region most effectively increases the aphelion dis-

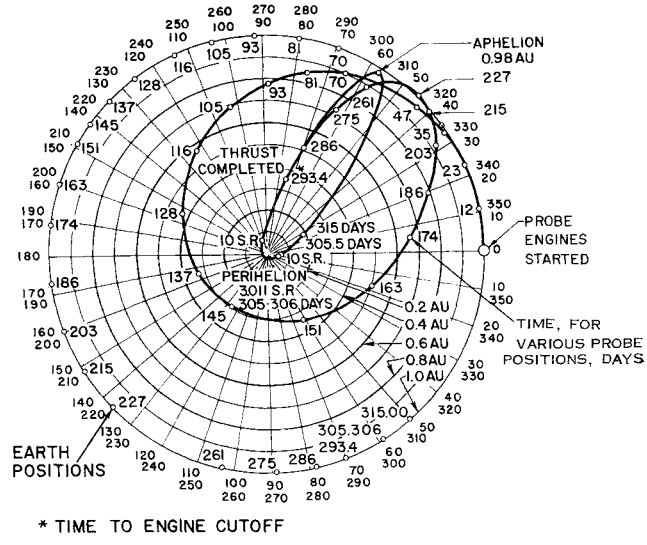

Fig. 3 Chosen trajectory: circumferential flip thrust + at $\ddot{r} > 0$; $-$at $\ddot{r} < 0$; $\alpha = 1.667$, $\beta = 0.1$.

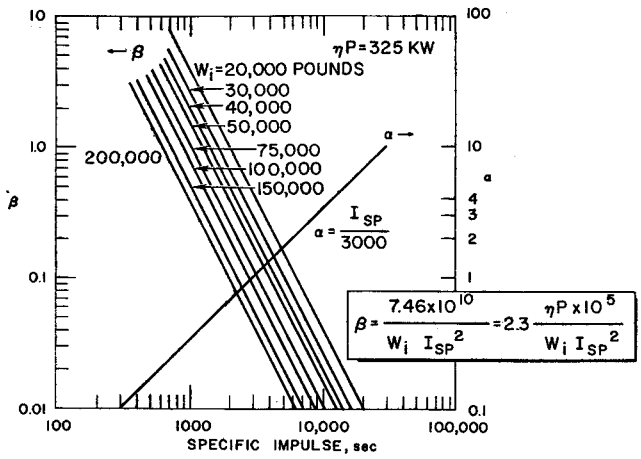

Fig. 4 Plot of nondimensional parameters α and β.

tance, whereas retrothrust in the plane of the trajectory applied as far from the sun as possible most effectively reduces the perihelion distance. From the point of view of guidance, this program has a considerable advantage over the other programs, since the thrust is always directed perpendicular to the probe-sun line in the plane of the trajectory.

The following relations between the system parameters are basic to the analysis of trajectories and propulsion:

Thrust

$$F = v_e \dot{W}_p/g_0 = I_{sp}\dot{W}_p \tag{5}$$

Beam Power

$$P_b = v_e^2 \dot{W}_p/2g_0 = g_0 I_{sp}^2 \dot{W}_p/2 \tag{6}$$

Initial Weight

$$W_i = W_d + (1 + \zeta)W_p \tag{7}$$

The nondimensional parameters α and β [Eqs. (4)] may alternatively be expressed by

$$\alpha = 0.330\, I_{sp}' \text{ and } \beta = 2.30\, P_b'/(I_{sp}')^2 W_i' \tag{8}$$

These parameters are plotted in Fig. 4 for a net beam power of 315 kw (415 kwe conditioned power input to an engine

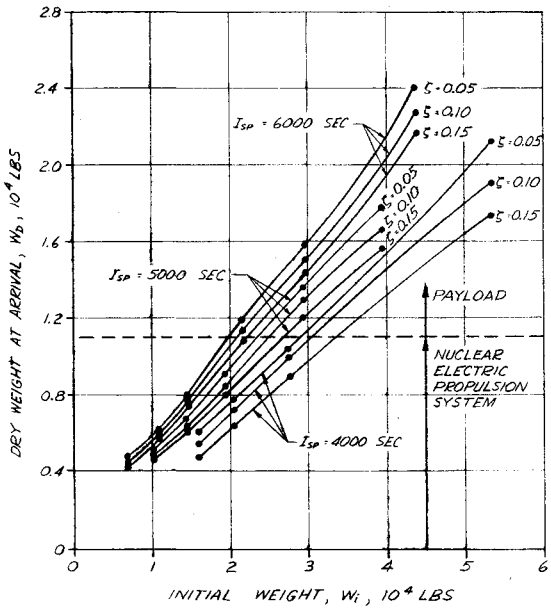

Fig. 5 For given powerplant: dry weight at arrival W_D (excluding tankage) vs initial weight W_i (approximate curves).

having an efficiency of 76%) for various values of specific impulse and initial weight. (These curves should be used as a guide only in that the engine efficiency, in general, will be a function of specific impulse.)

From the preceding equations, relationships are obtained for the following:

Beam Power to Initial Weight Ratio

$$(P_b/W_i) = 4\alpha^2\beta \tag{9}$$

Fraction of Propellant Consumed (in time t', sec)

$$(W_f/W_i) = 2(10)^{-7}\,\beta t' \tag{10}$$

Dry Weight Fraction (including tankage)

$$(W_d'/W_i) = 1 - 2(10)^{-7}\beta t' \tag{11}$$

Dry Weight Fraction (excluding tankage)

$$(W_d/W_i) = 1 - 2(10)^{-7}(1 + \zeta)\beta t' \tag{12}$$

The equivalent free-space velocity increment is

$$\Delta v = -\alpha \ln(1 - \beta t) \tag{13}$$

From a systems point of view, the goal is to find a set of parameters α and β with a thrust program such that the required ratio of thrust or beam power to the gross dry payload P_b/W_d is minimized within the requirements placed on the trajectory. The constraints include the requirement that the total propulsion time should be less than 1 yr (6.3 nondimensional time units) to achieve a feasible reliability requirement. Since the power supply of the propulsion unit will not work efficiently if too close to the sun, the trajectory must be chosen so that the radial distance from the sun is greater than some minimum value (for example, 0.1 a.u. or 20 solar radii) at all times during the thrusting period.

For a given specific impulse and a given powerplant, the beam power of the engine is fixed. Under these conditions the parameter beta is inversely proportional to the initial weight only. For given initial weights W_i and tankage factor ζ, the final dry weights, excluding tankage, were calculated and plotted in Fig. 5. The dotted line on this plot represents the weight of the nuclear-electric propulsion system. The region below the line has no physical significance, since it implies a "negative" net payload weight. The region above the dotted line represents an increasing payload for increasing dry weights at arrival.

The approximate upper limit on the initial weight is determined by the one-year maximum time of flight requirement.

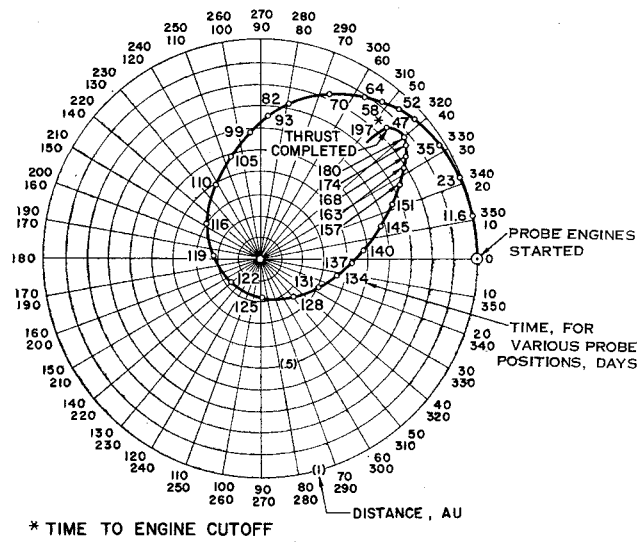

Fig. 6 Trajectory for low values of initial weight: circumferential flip thrust + at $\ddot{r} > 0$; − at $\ddot{r} < 0$; $\alpha = 1.667$, $\beta = 0.15$.

The limits are approximately

$I_{sp} = 4000$ sec	$W_{i\,max} = 5 \times 10^4$ lb
$I_{sp} = 5000$ sec	$W_{i\,max} = 4 \times 10^4$ lb
$I_{sp} = 6000$ sec	$W_{i\,max} = 3 \times 10^4$ lb

An analysis of the computer runs, furthermore, indicates that the region of optimum values of β within the allowable limits decreases slightly with increasing specific impulse as follows:

$I_{sp} = 4000$ sec	$\alpha = 1.33$	β(optimum) $= 0.131$
$I_{sp} = 5000$ sec	$\alpha = 1.67$	β(optimum) $= 0.1$
$I_{sp} = 6000$ sec	$\alpha = 2.00$	β(optimum) $= 0.094$

The chief objection to systems having high values of β is that these have very small initial weights and, consequently, low payloads. An example of this type of trajectory is shown in Fig. 6; it is not acceptable because it provides no payload with the postulated nuclear-electric propulsion system. The case shown in Fig. 7 provides for an adequate payload, but it is unacceptable for reasons of thermal control, because the spacecraft passes within 0.1 a.u. of the sun during the propelled period.

A feasible set of trajectory parameters for a probe with a final perihelion distance of 0.014 a.u. (three solar radii) is $\alpha = 1.67$ and $\beta = 0.1$ (Fig. 3). From the preceding equations, the specific impulse will be 5000 sec, and the ratio of beam power to initial weight will be 0.011 kw/lb. At a beam power of 315 kw and a tankage factor of $\zeta = 0.1$, the resulting parameters for the spacecraft are initial weight (W_i) = 28,340 lb (including a 1450-lb orbiter), weight of propellant (W_p) = 14,310 lb, and weight of tankage (ζW_p) = 1430 lb.

At 5.05 time units (approximately 293 days), the trajectory parameters are such that cessation of thrust results in an orbit with a perihelion of 0.014 a.u. At this time, the orbiter is separated from the propulsion unit. After separation, the orbiter reaches final perihelion in approximately 12 days. The orbiter is within 10 solar radii of the surface of the sun (the region of maximum scientific interest) for 9.6 hr during which time its nearest approach to the sun is to a perihelion of 3.011 solar radii (from the center of the sun). During the elapsed time of 2.09 days, which it takes the probe to complete the portion of the orbit within 20 solar radii, the earth moves about 2° relative to the sun. The communications-blackout cone (Fig. 8), which is defined as the region in which the solar radio noise increases by 50°K, is shown somewhat

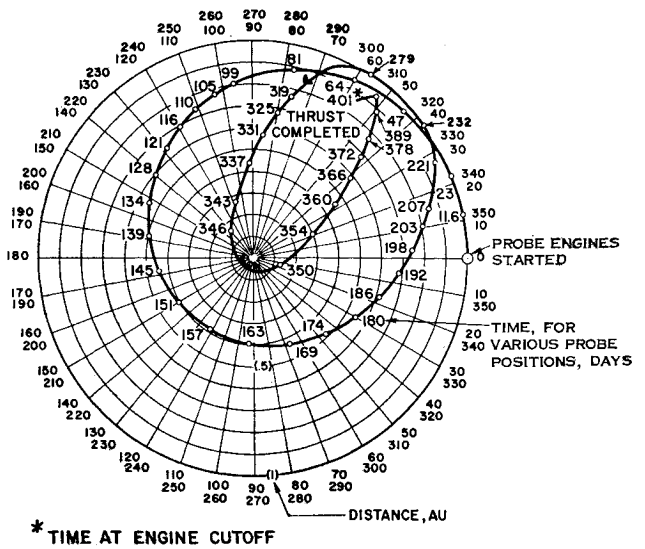

Fig. 7 Trajectory for high values of initial weight: circumferential flip thrust + at $\ddot{r} > 0$; − at $\ddot{r} > 0$; $\alpha = 1.667$, $\beta = 0.05$.

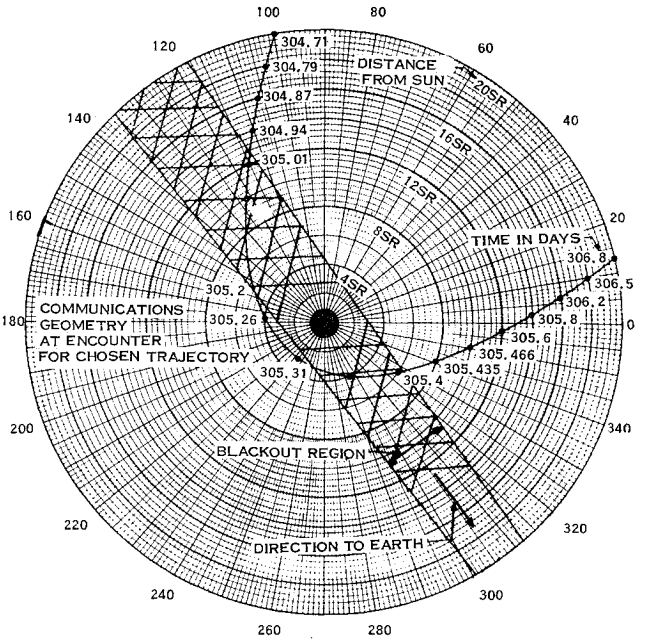

Fig. 8 Region of communication blackout due to radio noise from the sun.

enlarged to take into account this motion. The probe first encounters the blackout region approximately 12.5 solar radii from the center of the sun and leaves this region at a distance of about 5 solar radii. The total time of the first period of blackout is 5.8 hr. Direct communication with the probe may be carried on from 5 solar radii through perihelion to 3.2 solar radii, providing a possible 2.4 hr of real-time data transmission. Communication then is lost for 2.4 hr as the probe re-enters the blackout region. Contact again is established at approximately 6.3 solar radii. This result is, of course, predicated on assumptions regarding the noise interference from the sun and could prove to be optimistic if the flyby occurs during a period of great solar activity.

The Spacecraft

The spacecraft[5] (Fig. 9) is the carrier of the orbiter and contains power, propulsion, attitude control, command, and communications systems. A nuclear turboelectric system generates 500 kw of electric power for the 315-kwe ion-beam engine as well as for all auxiliary and communications equipment. The SNAP-50-type power system utilizes the Rankine cycle to generate the 500 kw of electrical power from a 3-Mw (thermal) nuclear reactor. The system itself is comprised of three major subsystems: the reactor-boiler heat source, the power conversion equipment, and the waste heat radiators. The direct-driven turboalternator generates 500 kw of

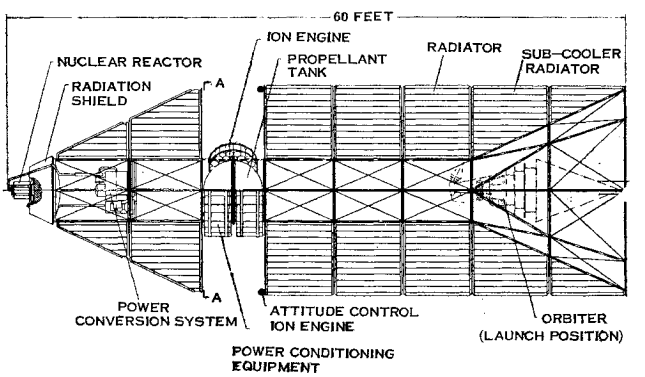

Fig. 9 The close-approach solar probe.

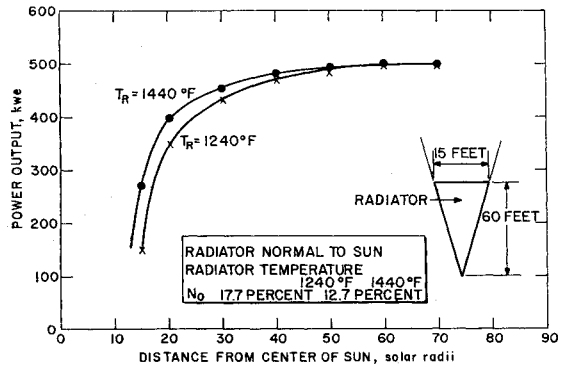

Fig. 10 Snap 50 system performance (without solar thermal shielding).

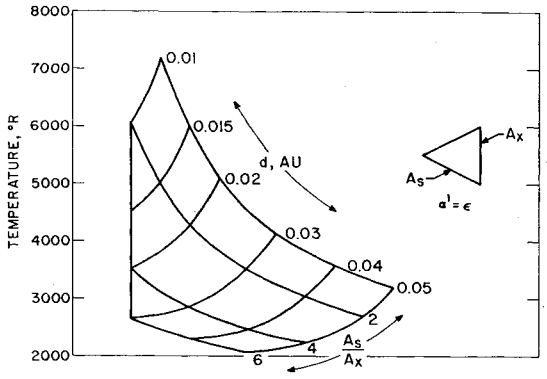

Fig. 12 Maximum first-shield equilibrium temperature as a function of distance and geometry.

three-phase, 2000-cps power at 3500 v. This is fed into the power-conditioning equipment (transformers, rectifiers, etc.) and is then distributed in appropriately conditioned form.

The primary radiator system for the rejection of waste heat from the cycle imposes certain restrictions on the distance to which the propulsion unit may approach the sun without thermal shielding. The predicted performance as the probe approaches the sun is shown in Fig. 10. The radiator temperature was kept constant in this analysis, a condition that results in a constant cycle efficiency. As the radiator begins to intercept heat flux from the sun, the heat power input from the Rankine cycle must decrease, requiring a reduction in the flow rate of the working fluid. This results in decreased electric power output. Assuming the system is capable of varying the working fluid flow rate over a wide range, the power output of the system without thermal shielding would be about as shown. The system will operate effectively without thermal shielding to about 20 solar radii. This imposes the restriction on the trajectory that the spacecraft must not pass closer to the sun than 20 solar radii while under thrust.

The unloaded spacecraft weights 11,150 lb. The cesium propellant weighs 14,300 lb, and the propellant tanks, 10% of this, or 1430 lb, whereas the payload or sun orbiter weighs 1450 lb. The total weight of 28,330 lb is the gross initial weight permitted by the desired trajectory. A separation system is provided for detaching the orbiter at the appropriate point in the trajectory after completion of the electric propulsion phase.

The Orbiter

During the powered phase of the mission, the requirements of the orbiter for power and communications are supplied by the spacecraft. However, when it is separated from the nuclear-electric ion propulsion system, it must be completely self-sufficient. It must have its own power supply, maintain proper attitude for the experiments and thermal control, and provide data handling and storage facilities as well as communications with earth.

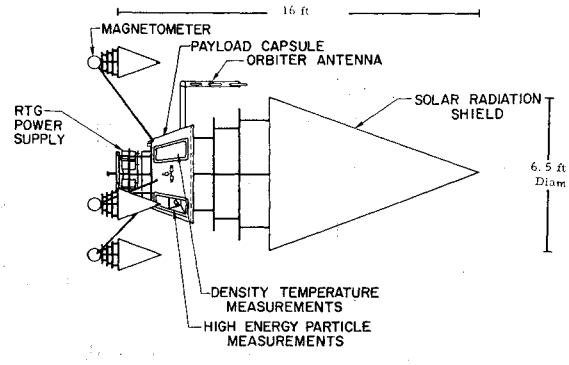

Fig. 11 Orbiter.

The concept of the orbiter (Fig. 11) is strongly influenced by the thermal shielding configuration and by the requirements of the experiments. The orbiter can tolerate the necessarily high temperatures for only relatively short times thus setting the requirements for a highly elliptical orbit. Analysis has shown that there is no need for the instruments to look through the solar radiation shield directly at the photosphere. The bulk velocity of the solar plasma (about 20 km/sec) and the velocity of the orbiter in the region within 10 solar radii (about 350 km/sec) are such that the apparent streaming direction of the plasma relative to the orbiter lies well outside of the thermal shield. Consequently, the solar plasma measuring devices may be housed in the shadow of the shield at all times.

Thermal Control

Since the transit time from earth's orbit to closest approach is about 10 months, it is desirable to have a passive thermal-control system based on radiation shielding, because the reliability of such a system is much greater than that of an active system. The shielding will reflect or reradiate a major portion of the incident solar flux, permitting only a small percentage to reach the payload. Regardless of the shielding design required to keep the heat input to the payload low, design requirements for the first shield (the shield receiving the direct solar flux) place a primary constraint on the minimum perihelion attainable. The major assumptions in our analysis include steady-state conditions, large isothermal regions, and gray bodies.

Consider a shield configuration that presents a greater surface A_s to the solar radiation than its cross-sectional area A_x. The maximum temperature of the shield may be determined from the relation

$$\alpha' A_x(r)^{-2} q_s = A_s \epsilon \sigma (T_{\max}')^4 \qquad (14)$$

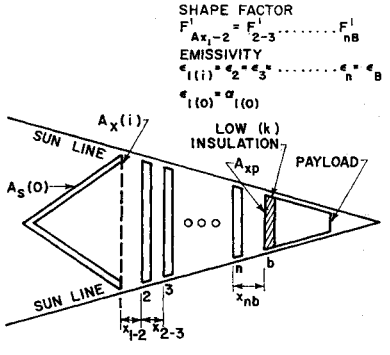

Fig. 13 Shielding system.

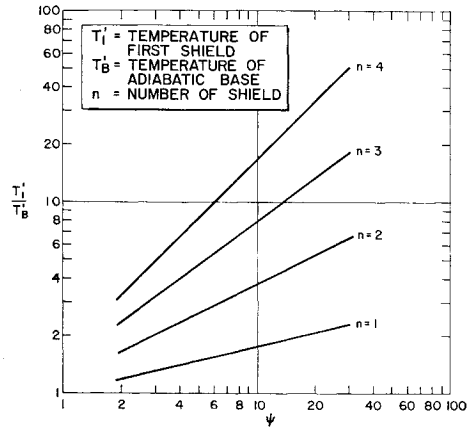

Fig. 14 Temperature ratio vs ψ.

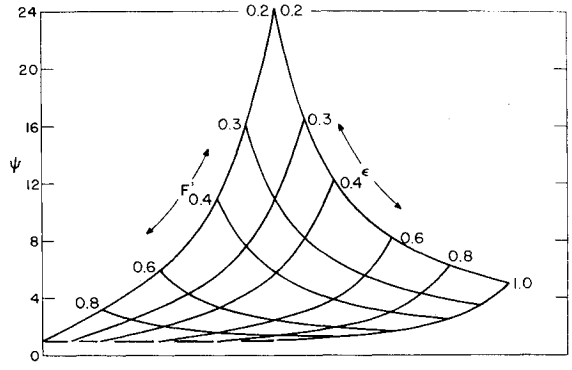

Fig. 15 ψ vs configuration factor and emissivity.

Since the operating temperatures in the region of interest are high, it is reasonable to assume that $\alpha' = \epsilon$ for the shield materials. (The maximum temperatures are plotted in Fig. 12 as a function of the shield ratio A_s/A_x and distance from the center of the sun.) The equation is applicable for orientation of either the base or vertex of the first shield toward the sun. It is clear that the first shield will operate at a temperature high enough to require the use of a refractory material such as tungsten. For example, at 0.014 a.u. the maximum temperature of a shield with an area ratio of three will be 4550 °R, or about 4100 °F.

Generally, if the first shield can be designed to withstand the severe thermal load, it is possible to have a shielding system that will protect the payload. However, it must be determined whether the design necessary for this protection of the payload is feasible within the size and weight restrictions of the over-all system. For example, for the arrangement of shields shown in Fig. 13, the number and spacing of shields necessary to keep the base of the capsule at an acceptable operating temperature must be determined. To do this, the following assumptions were made: 1) adiabatic wall at payload face B in Fig. 12, 2) equal shield emissivities, and 3) equal configuration factors between consecutive shields. Then the ratio of the temperature of the first shield to that of the adiabatic wall is equal to the fourth root of a function of the number of shields and the emissivity-configuration function, or

$$(T_i'/T_b')^4 = f(n, \psi) \tag{15}$$

The functional relation between T_i'/T_b', n, and ψ is plotted in Fig. 14, from which one can obtain numerical values of the shield parameter for several shield arrangements. With the shield parameter and the number of shields, and assuming an appropriate value for the emissivity ϵ, the value of the configuration factor F' is calculated from the expression,

$$\psi = (1 - F'^2 + \epsilon F'^2)/\epsilon F' \tag{16}$$

or it is obtained from Fig. 15. Since the configuration factor is a function of spacing and radius of the intermediate shields, values of the configuration factor have been plotted for values of this ratio (x/R) in Fig. 16. From the geometry of the conical shadow at closest approach (cone half-angle is approximately 20° at three solar radii), the permissable primary shield diameter, and the number of intermediate shields, their spacing can be determined keeping in mind that, for conservative design, the radius R referred to in the ratio x/R is the radius of the nth shield when the space is the nth space from the primary shield. To sum up, the procedure for determining the shield geometry is as follows: 1) determine an acceptable value of the adiabatic wall temperature T_b'; 2) determine the temperature of the first shield T_i', and calculate the ratio T_i'/T_b' (Fig. 12); 3) from Fig. 14, determine appropriate values of n and ψ; 4) from Fig. 15 (or the equivalent equation) and an appropriate value of ϵ, determine F'; 5) from Fig. 16 and F', determine x/R; 6) from the shadow geometry and the diameter of the primary shield, successively determine the spacings of the shields.

An inspection of the curves shows that, as the spacing increases, the number of shields required for a given degree of protection decreases. This must be balanced against the limited space available for shielding the payload due to the large angle of the shadow cone at closest approach as shown in Fig. 13.

As an example of the shielding system necessary for a close approach, consider the following conditions: $r = 0.014$ a.u., the allowable operating temperature of the base T_b is 1520 °R, the emissivity of all shields is $\epsilon = 0.4$, and the primary shield has an area ratio of $A_s/A_x = 3$. Then one obtains $T_i' = 4550$ °R, $T_i'/T_b' = 4550/1520 = 3$, $\psi = 2.75$ for $n = 3$ shields or $\psi = 6.5$ for $n = 2$. Furthermore, $F' = 0.670$ for $n = 3$, or $F' = 0.375$ for $n = 2$, and $x/R = 0.4$ for $n = 3$, or $x/R = 1.05$ for $n = 2$.

Since the primary shield has a diameter of 6.5 ft, the spacings x and base diameters D_b are as shown in Table 1. The choice would be the three-shield configuration because of the larger payload base diameter and volume. The length of the front shield is 9.2 ft, so that the length of the shield configuration including the base shield is 12.6 ft. This is the radiative heat shield. The maximum payload capsule base diameter is 4.04 ft, and the distance from the payload base to the tip of the shield shadow cone is about 5.55 it.

Table 1

	$n = 3$	$n = 2$
x_{12}	1.30 ft	3.41 ft
x_{2s} or $2b$	1.11 ft	1.96 ft
x_{3b}	0.95 ft	...
Σx_{ii}	3.36 ft	5.37 ft
D_b	4.04 ft	2.58 ft

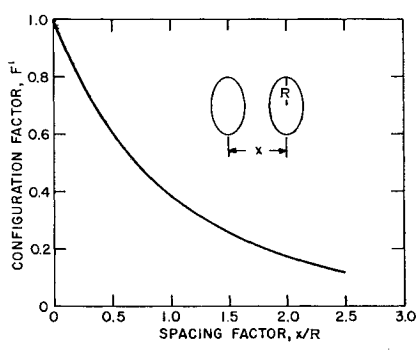

Fig. 16 Configuration factor as a function of geometry.

There are several general requirements that must be considered for the proper thermal design of the payload.

1) The internally generated heat to be dissipated places a constraint on the design since there must be sufficient radiating surface of the capsule to remove this energy (plus the heat leaked from the shielding system) at a low temperature.

2) The radiating surface must have a free view of space with the vehicle attitude controlled so that the solar flux never is incident directly on it.

3) The conduction paths from high-temperature sources to the payload must be restricted with the effective use of low-conductance insulation.

4) The temperature of the electric components must be held within a narrow band during any operation period.

An energy balance on the payload capsule results in

$$A_{xp}(k_i/\Delta x_i)(T_b' - T_p') + Q_p = A_{sp}\epsilon_p\sigma T_p'^4 \quad (17)$$

where the subscript p refers to payload.

For a typical example of the required surface area A_{sp}, take $T_b = 1520$ °R, $Q_p = 1$ kw = 3413 Btu/hr, T_p', max = 160 °F = 620 °R, $A_{xp} = 12.7$ ft², and $\epsilon_p = 0.9$. This results in $A_{sp} = 14.9 + 49.8\ (k_i/\Delta x_i)$ ft.² Using a multilayer, reflective vacuum insulation with a thermal conductivity of 0.002 Btu/hr-ft-°F, a 0.1-ft thickness of this insulation will require 15.9 ft² of radiating surface. Using a mineral fiber insulation with a conductivity of 0.03 Btu/hr-ft-°R, a thickness of 0.33 ft will require 19.4 ft² of radiating area. At a distance far removed from the sun, the minimum operating temperature of the payload capsule can be determined by setting the first term in the energy balance equation equal to zero.

The payload capsule design representative of the foregoing results is shown in Fig. 11. The cone frustrum area is 21.3 ft² which, when the reflective insulation is used, provides extra area to offset the thermal radiation from the magnetometer heat shields and the thermal resistance between the capsule components and its radiating skin. The radioisotope thermionic generator used in this solar probe concept has a substantially constant net output of 0.5 kw. This characteristic makes it possible to maintain close temperature control in the payload capsule by switching power not drawn by capsule components to dummy loads.

Materials

The selection of materials suitable for exposure to direct solar radiation at a few solar radii is one of the critical problem areas for this system. Ablative shielding was not considered applicable to the orbiter system. Tungsten is the current choice of material for components exposed to direct solar radiation. For intermediate shields, the maximum temperature is the primary constraint on material selection. The choice of materials, coatings, and finishes widens as the temperature decreases. Environmental-temperature effects on materials at a few solar radii from the sun and follow-up materials development are major areas for further study. An area of particular interest is the development of stable primary-shield surfaces with different emissivities on the solar and shadow sides.

Configuration

The resulting orbiter configuration has an over-all length of 16 ft and a maximum diameter of 6.5 ft. The primary thermal shield is 6.5 ft in diameter, and the entire thermal radiation shield is approximately 12.5 ft long, leaving for the instrument capsule a truncated cone of about 4.0-ft base diameter by about 1.9 ft long. All scientific instruments other than magnetometers are packaged within this volume along with data processing, data storage, transmitting and receiving, and power control equipment. The surface of the capsule radiates to space the heat generated by the equipment and leaked from the shield and power supply in order to maintain a temperature of less than 160 °F within the capsule. Packaged to the rear, a radioisotope thermionic generator supplies 500 w of primary power to the power-conditioning equipment in the capsule. Finally, to the rear of the generator, a small parabolic antenna with a gain of 20 db is mounted to provide an auxiliary means of communications should the primary antenna array be incapacitated during the final pass around the sun. Attitude is maintained by inertia wheels with solar pressure vanes to provide desaturation torques.

The entire orbiter is stowed within the probe (Fig. 9) during launch and after separation from the booster is deployed as shown. Separation of the orbiter from the main propulsion system is initiated by command from earth at the cessation of thrust.

Two antennas are shown: 1) a broadbeam, Yagi-type array for general communication during approach and encounter, and 2) a backup antenna located in the shadow of the orbiter. This latter antenna has a favorable look angle toward earth as the orbiter recedes from its solar encounter.

The breakdown of the 1450 lb allows approximately 600 lb for the thermal radiation shield, 300 lb for the structure, 170 lb for the power supply, 80 lb for experiments, and 300 lb for power conditioning and communications.

Power Supply

The criteria for the selection of a suitable power supply for the orbiter limited consideration to sun-powered thermoelectric converters, sun-powered thermionic converters, and radioisotope-powered thermionic converters. The radioisotope-thermionic converter system was selected for the main power supply.

Attitude Control

Attitude-reference signals may be obtained about two axes from sun sensors, whereas the third axis reference may be obtained from the star Canopus. Control torques during powered periods of flight can be supplied by ion-engine thrust vectoring in at least two axes and possibly all three axes. Control of the orbiter by mass-expulsion devices must be ruled out since this would contaminate the atmosphere (plasma) around the orbiter. Therefore, momentum wheels with solar desaturation torqueing devices will be used for controlling the attitude of the orbiter.

Communications

The feasibility of communications with the probe has been examined for both command and telemetry modes. Examination of these functions was made in terms of the closeness of the earth-probe line of sight to the sun, probe velocities as projected to line of sight (rate of change of doppler shift), communications range, and available time for transmission of data and reception of command. Command will present no difficulty even at the far reaches of the trajectory if one assumes the use of the 210-ft deep-space instrumentation facility (DSIF) antenna and some probable improvements in command receivers. Several periods of superior conjunctions occur during the trajectory, but since these conjunctions are of relatively short duration and at noncritical periods, it is not anticipated that these will impose significant communications restrictions.

The interval from final separation up to blackout at superior conjunction will initiate the primary scientific mission. It is desired that an effort be made to extract as much information as possible and transmit it to earth prior to the first near-perihelion blackout. Blackout due to a superior occlusion occurs at a starting time of approximately 305 days, when the probe is at a distance of approximately 12.5 solar radii. (The beginning of blackout is defined as an increase of sun-noise in the DSIF equal to 3 db. This is taken

as a noise temperature increase of 50 °K.) Blackout periods are shown in Fig. 8. The estimated engineering and scientific data rate requirement is appproximately 50 bits/sec.

It appears that an antenna of moderate gain can be used. It cannot be protected by the heat shield and still be effective for communications, since the earth sight angle with respect to the probe to sun line varies from only 25° to 30° down to nearly zero at blackout. A simple conceptual form could be a single or double stacked Yagi array, or a form of surface wave, endfire dielectric (possibly ceramic) antenna. The former, of metal, must be of tungsten or similar refractory material to withstand the temperature. The array would have approximately the following characteristics: gain, 12 to 15 db; beamwidth, 50° at 3-db points; and length, 2λ (10 in.) and, if stacked, 0.7λ between elements.

With an orientation such that maximum gain occurs near probe separation, as the earth-sun edge angle closes, a falloff in gain is experienced. This amounts to about 2.3 db, which closely approximates the increase in communications link gain due to the corresponding range decrease of from 1.3 to 1.0 a.u. Thus, relatively constant link gain is accomplished without need of a tracking antenna.

An examination of the power required to transmit 50 bits/sec through this interval yields a constant power requirement of approximately 190 w throughout the first phase with only a single initial orientation of the wide-beam antenna.

The second phase contains the heart of the data gathering mission; during this phase the orbiter goes through its point of closest approach to the sun, and thus this period is of maximum scientific interest. This period contains both a superior and inferior optical conjunction (in that order) of the sun with respect to the earth-orbiter line. The blackout period reduces the available real-time data transmission possibilities during this phase. In spite of the high scientific interest during this phase, real-time transmission of data therefore will be curtailed severely. The data collected during the optical and radio conjunctions must be recorded and stored for transmission after emergence from each total conjunction. A total of some 10×10^6 bits, which are to be collected through the period of the double conjunctions and closest sun approach, must be stored. The required tape recorder will need approximately 10 w on record and 1.5 w on playback; it is estimated to weigh ~25 lb and to occupy ~500 in.^{3} An effort should be made to transmit data during the "window" region between superior and inferior conjunctions. These data would consist of stored data obtained during superior conjunction and real-time data as obtained during the window time. Assuming a linear relationship between bits and mission time, this is some 8×10^6 bits in this region (with 10×10^6 bits total across the double conjunctions). The period of visibility is some 3.1 hr long between the points where sun noise in the DSIF has doubled. Converted to bits/sec, the 8×10^6 bits in 3.1 hr (11,200 sec) is some 710 bits/sec. The total power required to accommodate this bit rate (with the previously proposed antenna) is of the order of 1420 w. Doppler considerations may increase this power requirement. Provisions have not been included in the sun orbiter to accommodate this bit rate. At the noise-doubling points (3-db increase in DSIF noise), there still will exist a 7-db margin, and it is possible that the transmission window time may be somewhat increased. However, because of the uncertainties of the sun noise data, it is considered more conservative to use only the 3-db point. The maximum time possible between the photosphere occlusions is 5.1 hr, but since this is a limit case (both occlusions requiring the antenna to look directly at the sun and one occlusion actually obscuring the probe from earth), this length of time can only be approached at best. It can be seen that, as the window is widened, the bit rate requirement drops linearly with time for a total fixed number of bits.

Phase three is considered the main period of low-error data transmission from the probe back to earth. It is established that the order of 10×10^6 bits are to be transmitted back to earth. Tens of days should be the maximum time utilized for the purpose of information transfer to earth because of reliability considerations.

The time function associated with probe antenna to earth line of sight introduces an additional restriction. Since this postemergence period is to provide extremely reliable data transmission to earth, the antenna for this period should remain in the shadow of the orbiter sun shield. Limits of plus and minus 90° from the orbiter to earth line of sight can be established. The mission times associated with these antenna angles are 305.3 and 314.2 days. Thus, a period of approximately 8.9 days is available, from this standpoint, for the information flow. The necessary bit rate is 13 bits/sec, requiring 40 w for transmission with paraboloidal antenna or the same type antenna as is used for the primary broadbeam antenna. Three or four indexed antenna orientations will be adequate with this beamwidth.

Recapitulation of Problem Areas

The most critical problem areas uncovered by this study are propulsion and thermal protection for the orbiter. Problems associated with power supply for the orbiter and communications appear to be significant but much less serious. The thermal-control and materials problems in the design of an orbiter to pass within two solar radii of the surface of the sun are very significant. Although the study indicates that the problems may be solved, much work remains to be performed in these areas. An important area for optimizing the scientific payoff is the design of suitable experiments and instrumentation. The perturbations of the probe upon the plasma around it and the effect of the probe upon the instruments should be carefully considered.

The propulsion problem, especially, will require continued attention. For the feasible class of trajectories to be valid, the SNAP-50-type powerplant not only must be available but must be built within the planned design limitations. The study of trajectories should be continued in order to determine how deleterious the effect of any degraded performance of the nuclear-electric power supply will be.

Continued trajectory studies also may be desired to optimize communications considerations. Although emphasis should be placed on the trajectory analysis, materials research, and thermal-control areas, study efforts should continue on communications, power supplies, and attitude control, as well, in order that all significant problem areas may be identified and brought to solutions.

References

[1] Gold, T., private communication, Cornell Univ., Ithaca, N. Y. (April 1964).

[2] Krook, M., private communication, Harvard Univ., Cambridge, Mass. (April 1964).

[3] Hill, P. R., "Cost optimizing multi-stage rockets," Astronautics 8, 40–43 (January 1963).

[4] Hall, C. F., Northwang, G. J., and Hornby, H., "Solar probes," Aerospace Eng. 21, 22–30 (May 1962).

[5] Beale, R. J., Speiser, E. W., and Womack, J. R., "Electric space cruiser for high-energy missions," J. Spacecraft Rockets 1, 19–25 (1964).